Solving the line-shape problem with speed-dependent broadening and shifting and with Dicke narrowing. II. Application

R. Ciuryło,[1,2] D. A. Shapiro,[3] J. R. Drummond,[1,*] and A. D. May[1,†]
[1]*Department of Physics, University of Toronto, 60 St. George Street, Toronto, Ontario, Canada, M5S 1A7*
[2]*Institute of Physics, Nicholas Copernicus University, Grudziądzka 5/7, 87-100 Toruń, Poland*
[3]*Institute of Automation and Electrometry, Siberian Branch, Russian Academy of Sciences, Novosibirsk 630090, Russia*
(Received 5 June 2001; published 5 December 2001)

We apply the formalism presented in a previous paper to calculate spectra of an isolated line with speed-dependent broadening. The translational motion is modeled on a rigid-sphere interaction and includes the effect of the mass of the perturber on the profile. We show that the density, the mass of the perturber, and the ratio of the optical to kinetic cross section all play a role in revealing or concealing (in the profile) the effects of broadening, which depend upon the speed of the active molecule.

DOI: 10.1103/PhysRevA.65.012502 PACS number(s): 32.70.Jz

I. INTRODUCTION

There is a growing body of experimental evidence (cf. [1,2]) showing that speed-dependent broadening and shifting [3,4] plays a measurable role in determining the profile of an isolated line. There is also evidence that the models used to describe the translational motion, including Dicke narrowing [5], are inadequate. Up to now, the shapes of Dicke-narrowed isolated lines were mostly analyzed using profiles in which the treatment of velocity-changing collisions is based on the soft collision model [6–9], or the hard collision model [10–13], or a combination of the two [14–19]. However, it was recently shown [19] that any combination of the soft and the hard-collision model (Rautian-Sobelman [14] or Keilson-Storer [20]) is insufficient since it does not properly take into consideration the role played by the mass of the perturber.

While the basic transport/relaxation equation that governs the line shape is known, there are no analytical solutions of this equation for physically realistic conditions. Based on experience with the Boltzmann equation (a similar but simpler equation), it is reasonable to claim that it will never be possible to find analytical solutions for the line shape of an isolated line under physically realistic conditions. Most of the well-known analytical expressions for the line shape (Doppler, Voigt, Lorentzian, etc.) result from making overly simplifying approximations to the master-transport/relaxation equation. On the other hand, exact numerical solutions of the equation are relatively easy to generate. In Ref. [21] (hereafter referred as part I) we presented a formal method for solving the equation numerically. This reduced the line-shape problem to the art of choosing a complete and infinite set of basis functions and determining how many of these were to be used. Here we implement the formalism by selecting a set and, by testing for convergence, determine a practical number of functions to be included. At this stage the problem is reduced to solving a finite set of coupled linear equations. Being numerical in nature, we must, if we are to examine solutions, pick specific input parameters. For the speed-dependent broadening and shifting we assume that the form established for CO-N_2 [22] is also appropriate for CO-Ar. We describe the translational motion using the velocity-changing collision operator for billiard balls (rigid or hard spheres) [23,24]. A billiard-ball model is often used in statistical mechanics to treat the translational motion [25,26]. For us the advantage of using a rigid-sphere interaction lies in the fact that the matrix elements of this velocity-changing collision operator are known for any ratio of the mass of the perturber to the mass of the active molecule [23,24]. Many parameters contribute to the final profile. In this paper we take ''slices'' in parameter space in order to determine what are the important parameters that reveal or conceal spectral evidence of speed-dependent broadening.

II. LINE SHAPE

As was shown in part I, the shape of an isolated line is given by

$$I(\omega)=\frac{1}{\pi}\,\mathrm{Re}\,c_0(\omega), \tag{1}$$

where $c_0(\omega)$ can be evaluated by solving the set of complex linear equations

$$\underline{\mathbf{b}}=\mathbf{L}(\omega)\underline{\mathbf{c}}(\omega) \tag{2}$$

for the coefficient $c_s(\omega)$. The subscript s is explained below. Here the column $\underline{\mathbf{b}}$ contains one in the position 0 and zeros in other positions, i.e. $[\underline{\mathbf{b}}]_s=\delta_{s,0}$, and the column $\mathbf{c}(\omega)$ consists of the coefficients $c_s(\omega)$, i.e. $[\underline{\mathbf{c}}(\omega)]_s=c_s(\omega)$. The matrix $\mathbf{L}(\omega)$ depends on the frequency ω and has the following form:

$$\mathbf{L}(\omega)=-i(\omega-\omega_0)\mathbf{1}+i\mathbf{K}-\mathbf{S}_D^f-\mathbf{S}_{VC}^f, \tag{3}$$

where $\mathbf{1}$ is the unit matrix, $[\mathbf{1}]_{s,s'}=\delta_{s,s'}$, $\mathbf{K}$ is the matrix that represents the Doppler shift, $[\mathbf{K}]_{s,s'}=\langle s|\vec{k}\cdot\vec{v}|s'\rangle$, $\mathbf{S}_D^f$ is the matrix that represents the dephasing collision operator

*Email address: jim@atmosp.physics.utoronto.ca
†Corresponding author. Email address: dmay@physics.utoronto.ca

$\hat{S}_D^f$, i.e. $[\mathbf{S}_D^f]_{s,s'}=\langle s|\hat{S}_D^f|s'\rangle$, and $\mathbf{S}_{VC}^f$ is the matrix that represents the velocity-changing collision operator $\hat{S}_{VC}^f$, i.e. $[\mathbf{S}_{VC}^f]_{s,s'}=\langle s|\hat{S}_{VC}^f|s'\rangle$. In our ''matrix element'' notation the matrix element $[\mathbf{A}]_{s,s'}$ of an operator $\hat{A}$ are given by $\langle s|\hat{A}|s'\rangle=(\varphi_s,\hat{A}\varphi_{s'})$, where the scalar product of functions, $a(\vec{v})$ and $b(\vec{v})$, is defined as $(a,b)=\int d^3\vec{v} f_m(\vec{v})a^*(\vec{v})b(\vec{v})$. Here the Maxwellian velocity distribution $f_m(\vec{v})$ equals $(\pi v_m^2)^{-3/2}\exp(-v^2/v_m^2)$, where $v_m=\sqrt{2k_BT/m_A}$ is the most probable speed of the absorber, m_A is the mass of absorber, k_B is Boltzmann's constant and, T is the temperature of the gas. The chosen basis functions $\varphi_s(\vec{v})$ are orthonormal $[(\varphi_s,\varphi_{s'})=\delta_{s,s'}]$ with $\varphi_0(\vec{v})=1$.

III. CHOICE OF ORTHONORMAL BASIS FUNCTIONS

For linear absorption by systems in thermal equilibrium, the transport/relaxation equation has axial symmetry about the wave vector $\vec{k}$. A convenient complete set of basis functions with this symmetry can be constructed from the Burnett functions $\psi_{nlm}(\vec{v})$ by setting $m=0$ (cf. Lindenfeld and Shizgal [23]). We write these as [24]

$$\varphi_{nl}(\vec{v})=N_{nl}(v/v_m)^l L_n^{l+1/2}(v^2/v_m^2)P_l(\vec{e}_k\cdot\vec{e}_v), \tag{4}$$

where

$$N_{nl}=\sqrt{\frac{\pi^{1/2}n!(2l+1)}{2\,\Gamma(n+l+3/2)}} \tag{5}$$

is a normalization factor and $\Gamma(\ldots)$ is the gamma-Euler function. The functions

$$L_n^{l+1/2}(x^2)=\sum_{m=0}^{n}\frac{(-1)^m\Gamma(n+l+3/2)}{m!(n-m)!\Gamma(m+l+3/2)}x^{2m} \tag{6}$$

are the associated Laguerre polynomials (sometimes these are called Sonine polynomials [27]) and x is the reduced speed of the active molecule, where $x=v/v_m$. The functions

$$P_l(y)=\frac{1}{2^l}\sum_{k=0}^{[l/2]}\frac{(-1)^k(2l-2k)!}{k!(l-k)!(l-2k)!}y^{l-2k} \tag{7}$$

are Legendre polynomials and $y(y=\vec{e}_k\cdot\vec{e}_v)$ is the cosine of the angle between the velocity vector $\vec{v}=v\vec{e}_v$ and the wave vector $\vec{k}=k\vec{e}_k$ ($\vec{e}_v$ and $\vec{e}_k$ are unit vectors). The functions $\varphi_{nl}(\vec{v})$ are also eigenfunctions of the collision operator for Maxwell molecules [23], i.e., for molecules with a repulsive potential that varies as $1/r^4$.

The basis functions given by Eq. (4) were used by Lindenfeld [24] to calculate the self-structure factor for a gas of hard spheres. In optical spectroscopy this is the shape of a line undergoing Dicke narrowing but no collisional broadening or shifting. Robert and Bonamy [28] used the $l=0$ subset of these basis functions to calculate the shape of a line in the high-density ($\vec{k}=0$) limit with speed-dependent broadening and shifting and with a velocity-changing collision operator described by the Keilson-Storer model [20]. A general and more realistic treatment requires the inclusion of $\vec{k}\cdot\vec{v}$ in the master equation, the use of a potential to determine a collision operator that reflects the role of the mass of the perturber in the kinematics of collisions and, of course, the use of a broader set of basis functions.

In numerical calculations one needs to limit the complete infinite set of basis function to a finite set. Our choice of a finite set consists of using a function with $n=0,\ldots,n_{\max}$ and $l=0,\ldots,l_{\max}$. The index s, introduced above, represents the pair n and l and enumerates our basis functions $[\varphi_s(\vec{v})=\varphi_{nl}(\vec{v})]$. For programing it is convenient to define s by $s=n+(n_{\max}+1)l$. In this case s ranges from zero to $s_{\max}$, where $s_{\max}=n_{\max}+(n_{\max}+1)l_{\max}$. There are $s_{\max}+1$ basis functions.

IV. MATRIX ELEMENTS

To carry out the line-shape calculations, it is necessary first to specify the operators $\hat{S}_D^f$ and $\hat{S}_{VC}^f$, and second to evaluate all of the elements of all of the matrices which occur in Eq. (3). In order to compare our new results with previous calculations we do this for the case in which the collisional broadening and shifting varies quadratically with the speed of the active molecule. Dicke narrowing, caused by velocity-changing collisions, is modeled by colliding billiard balls with a specified mass ratio. Since the matrix elements of $i(\omega-\omega_0)\mathbf{1}$ are trivial, we move on to consider the other terms in Eq. (3).

If the Doppler shift $\vec{k}\cdot\vec{v}$ is written as $\omega_D\vec{e}_k\cdot\vec{v}/v_m$, where $\omega_D=kv_m$, then the matrix elements of $\mathbf{K}$ can be written as

$$[\mathbf{K}]_{nl,n'l'}=\omega_D\langle nl|\vec{e}_k\cdot\vec{v}/v_m|n'l'\rangle. \tag{8}$$

Using our basis functions $\varphi_{nl}(\vec{v})$, the elements $\langle nl|\vec{e}_k\cdot\vec{v}/v_m|n'l'\rangle$ can be calculated analytically and are given by

$$\begin{aligned}\langle nl|\vec{e}_k\cdot\vec{v}/v_m|n'l'\rangle=&[\sqrt{n+l+3/2}\,\delta_{n,n'}-\sqrt{n}\,\delta_{n,n'+1}]\\&\times\sqrt{\frac{(l+1)^2}{4(l+1)^2-1}}\delta_{l,l'-1}\\&+[\sqrt{n+l+1/2}\,\delta_{n,n'}-\sqrt{n+1}\,\delta_{n,n'-1}]\\&\times\sqrt{\frac{l^2}{4l^2-1}}\delta_{l,l'+1}.\end{aligned} \tag{9}$$

Next consider the matrix elements of the broadening and shifting operator $\hat{S}_D^f$. We recall from part I (in the case when velocity-changing and dephasing collisions are uncorrelated) that it is conventional to write the dephasing collision operator $\hat{S}_D$ as

$$\hat{S}_D=-\Gamma(v)-i\Delta(v), \tag{10}$$

where v is the speed of the active molecule. In part I we showed that the two operators $\hat{S}_D$ and $\hat{S}_D^f$ are identical. The calculations are simplified if we note that the matrix elements of the speed-dependent collisional width $\Gamma(v)$ and shift $\Delta(v)$ can be calculated numerically using the following relationship:

$$\langle nl|\Gamma(v)+i\Delta(v)|n'l'\rangle=\frac{4}{\sqrt{\pi}(2l+1)}N_{nl}N_{n'l}\delta_{l,l'}\times\int_0^\infty dx\, e^{-x^2}x^{2l+2}\times L_n^{l+1/2}(x^2)L_{n'}^{l+1/2}(x^2)[\Gamma(xv_m)+i\Delta(xv_m)]. \tag{11}$$

As in Refs. [9,19] we assume that the collisional width and shift vary as the square of the absorber speed [22] and are written in the form

$$\Gamma(v)+i\Delta(v)=\Gamma_0\left[1+a_W\left(\frac{v^2}{v_m^2}-\frac{3}{2}\right)\right]+i\Delta_0\left[1+a_S\left(\frac{v^2}{v_m^2}-\frac{3}{2}\right)\right], \tag{12}$$

where the parameters a_W and a_S control the magnitude of the speed dependence of the collisional width and shift, respectively. In this case we find

$$[\mathbf{S}_D^f]_{nl,n'l'}=-[\Gamma_0(1-a_W3/2)+i\Delta_0(1-a_W3/2)]\delta_{n,n'}\delta_{l,l'}-[\Gamma_0a_W+i\Delta_0a_W]\langle nl|v^2/v_m^2|n'l'\rangle, \tag{13}$$

where the elements $\langle nl|v^2/v_m^2|n'l'\rangle$ can be calculated analytically. They are given by

$$\langle nl|v^2/v_m^2|n'l'\rangle=[(2n+l+3/2)\delta_{n,n'}-\sqrt{(n+l+1/2)n}\,\delta_{n,n'+1}-\sqrt{(n+l+3/2)(n+1)}\,\delta_{n,n'-1}]\delta_{l,l'}. \tag{14}$$

Finally we consider the matrix elements of the velocity-changing collision operator $\hat{S}_{VC}^f$. The choice of rigid spheres as a model for the interaction permits us to compare our results with the recent treatment of Dicke narrowing [37] and earlier statistical calculations [24] using the same interaction. Perhaps, what is more important is the fact that Lindenfeld and Shizgal [23] have given analytical expressions for the matrix elements of the rigid-sphere velocity-changing collision operator for the same basis functions as used here. Following Lindenfeld [24] we can write

$$[\mathbf{S}_{VC}^f]_{nl,n'l'}=\nu^{(0)}M_{nl,n'l'}^{E*}, \tag{15}$$

where $\nu^{(0)}=v_m^2/(2D^{(0)})$ and

$$D^{(0)}=\frac{3}{8}\left(\frac{k_BT}{2\pi\mu}\right)^{1/2}\frac{1}{N\sigma^2} \tag{16}$$

is the first-order self-diffusion coefficient for rigid spheres. Here σ is the average of the rigid-sphere diameter of the absorber and perturber, N is the number density of perturbers, $\mu=m_Am_P/(m_A+m_P)$ is the reduced mass, m_A is the mass of the absorber, and m_P is the mass of the perturber. The coefficients $M_{nl,n'l'}^{E*}$ are given by the following equation [23,24]:

$$M_{nl,n'l'}^{E*}=-\delta_{l,l'}\frac{3\,l!}{8M_2}\sqrt{\frac{n!n'!}{\Gamma(n+l+3/2)\Gamma(n'+l+3/2)}}\left\{\sum_{p=0}^{\tilde{n}}\sum_{s=0}^{\tilde{n}-p}\sum_{m=0}^{\tilde{n}-p-s}\sum_{q=0}^{l}\sum_{r=0}^{l-q}\left[\frac{4^p(r+s+p+q+1)!}{(p+q+1)!r!s!}\right]\times\left[\frac{\Gamma(n+n'-2s-2p-m+l-r-q-1/2)B_{p,q}^{(1)}(\infty)}{(n-m-s-p)!(n'-m-s-p)!(l-r-q)!m!}\right][M_1^{l+p-r-q}M_2^{n+n'+q-2m-2s-p}(M_1-M_2)^{m+r+2s}]\right\}, \tag{17}$$

where $M_1=m_A/(m_A+m_P)=1-M_2$, $\tilde{n}=\min(n,n')$ and

$$B_{p,q}^{(1)}(\infty)=\frac{(2p+q+1)!}{2q!(2p+1)!}-\frac{2^{q-1}(p+q+1)!}{p!q!}. \tag{18}$$

For the M_1 or M_2 equal to zero, and for $M_1=M_2$ the coefficients occurring in Eq. (15) are defined as $\lim_{M_1\to0}M_{nl,n'l'}^{E*}$, $\lim_{M_2\to0}M_{nl,n'l'}^{E*}$, and $\lim_{M_1\to M_2}M_{nl,n'l'}^{E*}$, respectively.

As discussed by Lindenfeld [24], the exact diffusion coefficient D differs from $D^{(0)}$. The ratio $f_D=D/D^{(0)}$ can be found by solving the following set of linear equations:

$$-\sum_{n'=0}^{\infty}M_{n1,n'1}^{E*}a_{n'}=\delta_{n,0} \tag{19}$$

for a_n. The ratio f_D is equal to a_0. By introducing f_D we can rewrite Eq. (15) in the form

$$[\mathbf{S}^{f}_{VC}]_{nl,n'l'} = \nu_{\rm diff}\, f_D M^{E*}_{nl,n'l'}, \tag{20}$$

where the effective frequency of velocity-changing collisions $\nu_{\rm diff}$ is defined by

$$\nu_{\rm diff} = \frac{v_m^2}{2D}. \tag{21}$$

The parameter $\nu_{\rm diff}$ is commonly used in the investigation of Dicke narrowed lines to characterize velocity-changing collisions.

This completes our discussion of evaluating the matrix elements for the set of coupled equations represented by Eq. (2). In the present case all matrix elements are analytical in form. Nevertheless, we solve the set of equations numerically, using standard software. We refer to the resulting line shape as a speed-dependent billiard-ball (SDBB) line shape.

V. CALCULATIONS AND RESULTS

The parameters that control the calculated line shape are the temperature T, the mass of the active molecule m_A, the mass of the perturber m_P, the wave vector $\vec{k}$, the kinetic cross section (hidden in $\nu_{\rm diff}$), the optical cross section (hidden in Γ_0 and Δ_0), and the amplitudes of the speed dependence of the collisional broadening and shifting, a_W and a_S. The parameters $\nu_{\rm diff}$, Γ_0, and Δ_0 are all proportional to the density, which is the last control parameter. It would be a formidable task to examine the anatomy of an isolated line over such an enormous parameter space. We, therefore, limit our examination primarily to the influence of the speed-dependent broadening on the line shape (a subject of current interest) and through the translational motion, the influence of the perturber to absorber mass ratio, $\alpha = m_P/m_A$, on the profile.

In the calculations we use the dimensionless variables, $u=(\omega-\omega_0)/\omega_D$, $g=\Gamma_0/\omega_D$, $d=\Delta_0/\omega_D$, and $z=\nu_{\rm diff}/\omega_D$, where ω_D is related to the Doppler width. As in Ref. [19] we consider conditions appropriate for infrared absorption by light molecules where the kinetic and optical cross sections are comparable. These are proportional to $\nu_{\rm diff}$ and Γ_0, respectively. Here we copy [9] and take $\nu_{\rm diff}/\Gamma_0$ equal to 1.14 and we ignore the shift by setting Δ_0 equal to zero. For the speed-dependent broadening, once again we copy [9] taking $a_W=0.1$. These are values appropriate for CO perturbed by a range of molecules and atoms [2,7,11,22] for which the collisional shift of the lines is very small. The remaining parameters are fixed at values appropriate to the fundamental band of CO at room temperature.

One aspect of the problem that we shall explore numerically is the influence of α on the line shape. It is known, as α goes to zero, that D reduces to D_0 and the SDBB profile reduces to the soft collision or speed-dependent Galatry line shape (SDG) [9]. The only aspect of the problem that reflects the choice of the interaction being for billiard balls is that D_0 is given by Eq. (16). Analytical expressions for the SDG profile [9] exist for the case where $\Gamma(v)$ is given by Eq. (12). We have used the comparison of spectra calculated for this SDG profile with our SDBB line shape with $\alpha=0$ to check for convergence of our calculations. We have shown that setting $n_{\max}=10$ and $l_{\max}=10$ gives a highly accurate line shape (convergence to within 10^{-6} of the peak value) and in a time much shorter than the iterative method used in Ref. [19].

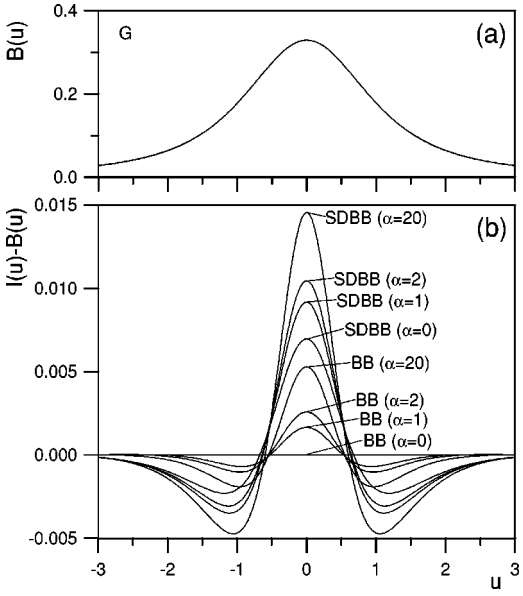

FIG. 1. Comparison of line shapes obtained for $\nu_{\rm diff}/\Gamma_0 = 1.14$, $g=0.7$, $d=0.0$, $z=0.8$, and $a_W=0.1$. (a) The base curve: Galatry profile G. (b) Differences between the calculated profiles and the base curve: BB-G and SDBB-G for $\alpha=0$, 1, 2, and 20.

While the influence of the speed-dependent broadening ($a_W\neq 0$) and of the finite mass of the perturber ($\alpha\neq 0$) on the spectral profile of an isolated line are readily detected experimentally (cf. [29–31]), they are nevertheless small in most cases. In order to show the presence of such an effect in our calculated profiles, we will display the lines as the difference between the calculated profile and some base or reference profile.

We first perform calculations at a density such that $z=0.8$ and take $g=0.7$. When g and z are near unity the influence of speed-dependent effects and of Dicke narrowing on the shape of spectral lines is significant. In this region of parameter space, Dicke narrowing is sensitive to the mass ratio α. On the scale of Fig. 1(a) all of the curves obtained by reducing a_W to zero or by varying α would be close together. Therefore, in Fig. 1(a) only the base curve $B(u)$, taken here as the speed-independent soft-collision or Galatry line shape G [6], is shown. In Fig. 1(b) we illustrate the sensitivity of the curves to the choice of mass ratio α and to the presence or absence of the speed-dependent broadening, by plotting $I(u)-B(u)$. The solid line at zero is for rigid spheres with $a_W=0$ and $\alpha=0$. That the speed-independent BB profile reduces to the soft-collision model for $\alpha=0$ is not surprising as any interaction potential leads to this result as the mass of the perturbers approaches zero. For $\alpha\neq 0$ but still for speed-independent broadening ($a_W=0$) we find, in order of increasing amplitude at zero frequency, the speed-independent BB profiles with $\alpha=1$, 2, and 20. For the speed-dependent profiles ($a_W=0.1$) we find, at the same density, that the zero-

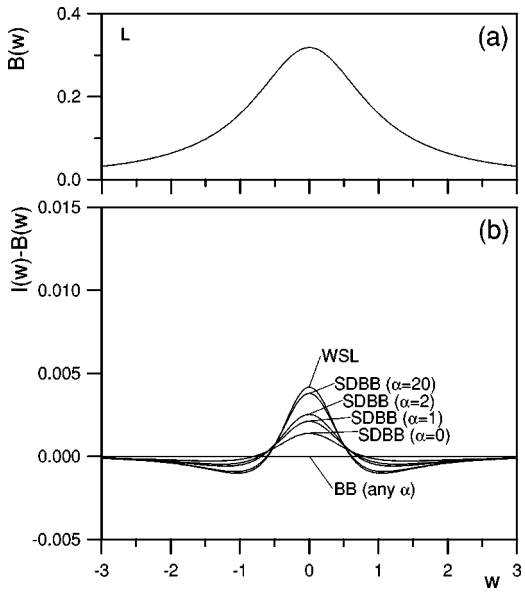

FIG. 2. Comparison of line shapes obtained in the hydrodynamic limit ($\omega_D=0.0$) for $\nu_{\rm diff}/\Gamma_0=1.14$, $\Delta_0=0.0$, and $a_W=0.1$. (a) The base curve: Lorentz profile L. (b) Differences between the calculated profiles and the base curve: SDBB-L for $\alpha=0$, 1, 2, and 20. The upper curve is a plot of WSL-L.

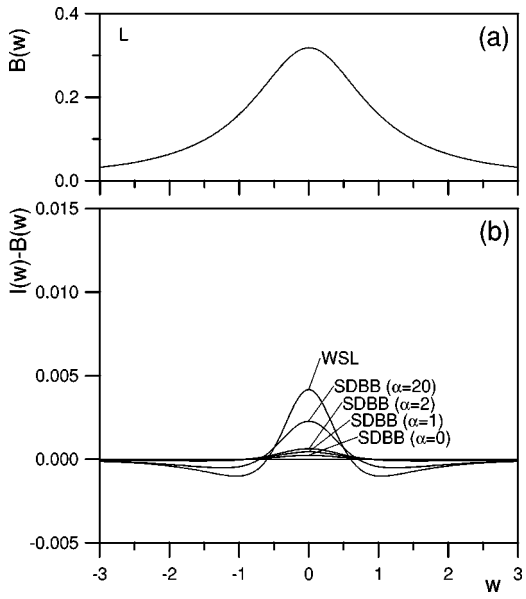

FIG. 3. Comparison of line shapes obtained in hydrodynamic limit ($\omega_D=0.0$) for $\nu_{\rm diff}/\Gamma_0=10.0$, $\Delta_0=0.0$, and $a_W=0.1$. (a) The base curve: Lorentz profile L. (b) Differences between the calculated profiles and the base curve: SDBB-L for $\alpha=0$, 1, 2, and 20. The upper curve is a plot of WSL-L.

frequency amplitudes lie higher than the results for the speed-independent profiles and in the same order with varying α. As mentioned earlier, the SDBB line shape with $\alpha=0$ is identical to the SDG line shape [9]. We have verified this numerically.

It is clear from Fig. 1(b) that departures from the soft-collision model arising (at low densities) from the nonzero mass of the perturber can be very similar to departures arising from speed-dependent broadening. However, the reader should keep in mind that we reach this conclusion by varying these two parameters while holding other parameters or conditions fixed at specified values. In another region of parameter space, varying the same two parameters could (and does) lead to different conclusions. Two important fixed parameters/conditions for Fig. 1 were density ($z=0.8$) and $\nu_{\rm diff}/\Gamma_0=z/g=1.14$.

Keeping $\nu_{\rm diff}/\Gamma_0$ equal to 1.14, we now examine the high-density or hydrodynamic regime. For large values of z, $\nu_{\rm diff}$ is much larger than $\omega_D=kv_m$ and the Doppler term $\vec{k}\cdot\vec{v}$ may be simply dropped from the transport/relaxation equation. In this collision-dominated regime we anticipate a density-independent line shape if the detuning is scaled with the density. As in Ref. [19] we define a reduced detuning w by $w=(\omega-\omega_0)/\Gamma_0$ and we set $\Delta_0=0$. In the high-density regime, the soft-collision base profile used for Fig. 1(b) reduces to a simple Lorentzian of width Γ_0. This base profile $B(w)$ is shown in Fig. 2(a). Departures from the base profile, $I(w)-B(w)$ as α and a_W are varied, are shown in Fig. 2(b). In contrast to Fig. 1(b), the departures for $a_W=0$ are zero for all values of the mass ratio and not just for the $\alpha=0$ case. With the speed-dependent broadening ($a_W=0.1$) the departures at zero detuning are ordered in the same way as in Fig. 1(b) for low densities. If the mass of the perturber was infinite (the so-called Lorentz gas), the active molecules would move with constant speed and each speed class would make a contribution to the spectrum that was a Lorentzian with a width $\Gamma(v)$. Consequently the profile should approach a weighted sum of Lorentzian (WSL) profiles [32] as α is increased. Departures of the WSL profile from the base Lorentzian are also shown in Fig. 2(b). As expected the rigid-sphere calculations appear to approach this limit as the mass ratio is increased. Below we will explore whether this is true in other regions of parameter space. Nevertheless, it is clear from Figs. 1(b) and 2(b) that departures from simple line shapes due to the speed-dependent broadening depends upon both the density and the mass ratio. We emphasize that the departures plotted in Figs. 1(b) and 2(b) are departures from a *prescribed* base profile and not (as is common in experimental papers) departures from a *fitted* (base) profile. Thus, for example, they are not to be compared with the residuals shown in [29].

We now explore a different section of parameter space. As in Fig. 2 we consider z to be large. We fix the speed-dependent broadening ($a_W=0.1$) and we calculate profiles with different mass ratios and different ratios of the kinetic to optical cross section (represented by $\nu_{\rm diff}/\Gamma_0$). In Fig. 3(a) we take, as a base profile, the same simple Lorentzian profile with width Γ_0 as shown in Fig. 2(a). The results for $\nu_{\rm diff}\gg\Gamma_0$, $\nu_{\rm diff}\ll\Gamma_0$, $\nu_{\rm diff}=10\Gamma_0$, and α equal to 0, 1, 2, and 20 are shown in Fig. 3(b). In the case of $\nu_{\rm diff}\gg\Gamma_0$ and for all values of α considered, the departures from a simple Lorentzian are zero. For the case of $\nu_{\rm diff}\ll\Gamma_0$ the departures are again independent of the mass ratio and are not distinguishable from those for the WSL, shown in Fig. 3(b). For $\nu_{\rm diff}$

$=10\Gamma_0$, the results fall between the first two cases, approaching a WSL's as α is increased. Note, at say $\alpha=20$, that the departures from the base spectrum shown in Fig. 2(b) for $\nu_{\rm diff}/\Gamma_0=1.14$ are almost a factor of 2 larger than those shown in Fig. 3(b) for $\nu_{\rm diff}/\Gamma_0=10$. Clearly, we must add the ratio of the kinetic to the optical cross section to the list of parameters that influence the degree to which the speed-dependent broadening will impact on the line shape. The same conclusion was reached earlier but was based on calculations with model collision kernels [19] as opposed to a model (BB) interaction potential.

It is easy to give a physical interpretation of the results shown in Fig. 3(b). In the case of $\nu_{\rm diff}\gg\Gamma_0$ the exchange between velocity classes is rapid. If the mass of the perturber is not large (compared to the mass of active molecule), this implies that the exchange between speed classes is also rapid with respect to the decay of the optical coherence (broadening). Thus it is appropriate to replace the latter term in the relaxation/transport equation by the average value of the width, $\int d^3\vec{v}\, f_m(\vec{v})\Gamma(\vec{v})$, i.e., by a value that is independent of the speed and, here, equal to Γ_0. Consequently the resulting profile is a simple Lorentzian (see Ref. [19]) and the departures vanish. The mass ratio (at least if it is finite) plays no role in this argument. However, beware. If α is very large (infinite), even if $\nu_{\rm diff}$ is large, velocity-changing collisions do not change the speed of the active molecule and in this case the resulting profile is a WSL. The range of α very large is not explored in Fig. 3(b).

In the reverse situation ($\nu_{\rm diff}\ll\Gamma_0$) the velocity and thus also the speed, relaxes slowly with respect to the optical coherence that therefore, decays at a constant speed. Consequently, in the hydrodynamic region, the profile will become a weighted sum of Lorentzians. Here, the mass ratio is irrelevant to the argument.

In the intermediate case ($\nu_{\rm diff}=10\Gamma_0$) the mass ratio plays a crucial role as it varies (for a given intermolecular interaction) the relative importance of speed changing versus direction changing collisions. Thus in Figs. 2(b) and 3(b), as the mass of the perturber increases, the velocity-changing collisions become more-speed-conserving collisions and thus the profile must approach closer to a WSL, the same limit that is reached for $\nu_{\rm diff}\ll\Gamma_0$. None of these general arguments are connected to the specific use of billiard balls as a model interaction potential but rather they are connected to basic kinematics and the general consequence of having a dynamic system in which there are both fast changing and slowly changing variables.

From Figs. 1–3 and their interpretation we reach the main conclusion of this paper. This conclusion states that the degree to which the speed-dependent broadening becomes apparent in the shape of an isolated line depends upon the density, the ratio of the kinetic to optical cross section and the ratio of the mass of the perturber to the mass of the active molecule. Any analysis of experimental profiles that does not include all of these factors will be flawed. For example, note that the observation that a line is a simple Lorentzian does not establish, on its own, that the broadening is speed independent. In this paper while our discussion is based on collisionally unshifted lines, the SDBB model can also be applied to strongly shifted lines, including the case where the perturber mass is greater than the mass of the active molecule [1,33,34].

Having reached our main conclusion, we move on to discuss the relation of the present paper to earlier work. Here we have considered the speed-dependent broadening and treated the translational motion by modeling the molecular interaction as for billiard balls (rigid or hard spheres). In the literature, different models for the velocity-changing collision operators have been used [6,10,14,20]. In general, none of these model-collision operators depends upon the ratio of the mass of the perturber to the mass of the active molecule. Of course, it is well known that any physically realistic interaction potential will lead to the soft-collision model [6] as the mass ratio goes to zero. The hard-collision model of Nelkin and Ghatak [10] is often presumed to be appropriate for treating the translational motion in the limit of α going to infinity. This is false. We have shown by direct comparison that in the hydrodynamic limit the speed-dependent Nelkin-Ghatak profile (SDNG line shape) [12,14] is close to the SDBB profile for $\alpha=1$. Under the same conditions, but with the speed-independent collisional broadening and shifting the BB line shape, for any value of α, is essentially the same as the corresponding speed-independent Nelkin-Ghatak profile. For the same conditions as in Fig. 1(b) we find that the SDBB profile with $\alpha=4$ agrees with the SDNG profile and in the speed-independent case that the BB profile with $\alpha=9$ closely mimics the NG profile. Clearly the hard-collision model for the collision operator does not mimic the collision operator for very heavy perturbers. The Keilson-Storer [20] and the Rautian-Sobelman [14] model for the velocity-changing collision operator also suffer from their inability to reflect the role of the mass of the perturber on the speed-dependent profile of an isolated line. On the other hand, as we have shown, even a simple model for the interaction potential does capture the essential dependence of the profile on the mass ratio. Furthermore, since the numerical steps required to go from a potential to a collision kernel to a collision operator are well understood, it is possible to carry out a full *ab initio* calculation of the translational motion and, of course, of the speed-dependent collisional broadening and shifting. Thus it is possible to carry out a semiclassical, *ab initio* calculation of the speed-dependent profile of an isolated line. This is our ultimate objective.

The self-structure factor for hard sphere gas was calculated much earlier by Lindenfeld [24] and after normalization is identical to our billiard-ball profile if the collisional broadening and shifting is neglected. We also note it is possible to solve analytically the billiard-ball transport equation for the Lorentz gas, i.e., for massive perturbers [35,36]. Indirectly, Lindenfeld [24] has raised the question, of how or if the BB line shape for a finite mass ratio approaches the Lorentz gas profile as $\alpha=m_P/m_A$ is increased towards infinity. The crux of the question deals only with the translational motion. We can examine the same question by performing calculations with $\Gamma_0=\Delta_0=0$. In fact we have checked our software by comparing our calculations with those presented in Lindefeld's paper [24] for small values of α. However, we can carry out numerical calculations (using $n_{\rm max}=30$ and

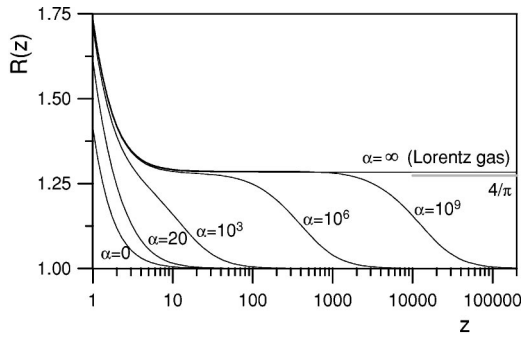

FIG. 4. Dependence of the normalized peak amplitudes R calculated numerically for $\alpha=0$, 20, 10^3, 10^6, 10^9, and ∞ (Lorentz gas) are plotted. The exact asymptotic value of $\lim_{z\to\infty} R_{\mathrm{anal}}(z) = 4/\pi$ for Lorentz gas is also marked on the plot.

$l_{\max}=10$) for large values of α, even for α equal to infinity. [This corresponding to $M_1=0$ and $M_2=1$ in Eq. (17).] Thus we can more thoroughly examine the question of as to how the finite mass calculations approach the Lorentz gas results. As a basis of the comparison we use

$$R=\frac{I_0}{J_0}, \tag{22}$$

a normalized peak amplitude. Here I_0 is the BB profile with $\Gamma=\Delta=0$ and $\omega=\omega_0$. The normalization factor J_0 is defined as the peak amplitude of a Lorentzian profile given by

$$J(\omega)=\frac{1}{\pi}\mathrm{Re}\frac{1}{\omega_D^2/(2\nu_{\mathrm{diff}})-i(\omega-\omega_0)}. \tag{23}$$

This has a Dicke width (half width at half maximum) [5] given by $k^2D=\omega_D^2/(2\nu_{\mathrm{diff}})=\omega_D/(2z)$ [5]. We know that R will approach a value of 1 for any finite value of α, as z approaches infinity since this is the translational hydrodynamic limit for any gas with the zero broadening and shifting. Using our numerical procedure it is a simple matter to calculate approximate but reasonable values of the peak amplitude of I_0 over a range of values of α and z. We can also calculate J_0 since D is also calculable [see Eq. (19)]. Thus we calculate R numerically for any α and z. Since analytical expressions of $I(\omega)$ exist for the Lorentz gas profile [24,35,36], it is also an easy matter to calculate R_{anal} for this case. The only difficulty here is that each speed class has its own diffusion constant $D(v)$ and we cannot automatically assign a value of ν_{diff} in Eq. (23). In a manner similar to that of Lindenfeld we use the quantity $D=\int d^3\vec{v} f_m(\vec{v})D(v)$ defined as the Maxwellian weighted average of $D(v)$ and through this we define a value of ν_{diff} and z. With this definition, Lindenfeld showed that R_{anal} for the Lorentz gas approaches a value of $4/\pi$ as z approaches infinity. As a check on our numerical procedure we calculated the Lorentz gas profile numerically and compare our $\lim_{z\to\infty} R(z)$ with the analytical value of $4/\pi$. As can be seen in Fig. 4 the agreement is sufficient to justify drawing qualitative conclusions from the figure. For large values of α (10^3, 10^6, 10^9, and ∞) the numerical errors are about 1%.

Figure 4 shows plots of R as a function of z for a range of values of the mass ratio α. We see that R calculated from the BB profile is close to the value of R calculated for $\alpha=\infty$ (Lorentz gas) only for large values of α and only over a limited range of z. The dependence of R on α is easily interpreted in the same manner as above. As α is increased, velocity-changing collisions become more and more solely direction-changing collisions, and at a given z, the curves must approach the Lorentz gas value with increasing mass ratio, i.e., must approach a weighted sum of Lorentzian profiles in which each Lorentzian component has a Dicke width given by $k^2D(v)$. However, for a fixed and finite value of α, the curves must eventually approach the full mathematical hydrodynamic value determined by a diffusion constant that includes the thermalization of the speed of a tagged particle. We have confirmed this interpretation by showing, in the plateau region of Fig. 4, that the calculated spectrum is indistinguishable from the weighted sum of Lorentzian profiles calculated for pure, but inhomogeneous Dicke narrowing. Thus, over a limited range of z, the BB and the Lorentz gas profile are nearly identical. However, the values of α and the range of z are such that it will be very difficult, if not impossible, to realize these conditions experimentally.

Finally, Shapiro and May [37] have also considered the case of the translational motion of rigid spheres. Since they discretized the velocity distribution function, in effect their basis functions were a series of δ-Dirac functions spread over the velocity. With this set of basis functions, they were able to carry out practical calculations only by reducing the collision kernel to one dimension. With the basis functions used here, full three-dimensional calculations can be performed on available PC's in a few seconds for the spectra shown in Figs. 1–3 (which contain 241 points evenly spaced for reduced detuning (u or w) from -3 to $+3$) with $n_{\max}=l_{\max}=10$. At lower densities, $n_{\max}$ and $l_{\max}$ must be increased to obtain convergence with a consequent increase of computation time by roughly the cube of $(s_{\max}+1)$. In this region, many terms are required to capture the Doppler (Gaussian) aspects of a line.

VI. SUMMARY AND CONCLUSION

In this paper, we have implemented the formalism presented in part I for the calculation of the spectral profile of an isolated line undergoing speed-dependent broadening and shifting with Dicke narrowing. Not only did the specific choice of basis functions, Eq. (4), permit us to calculate, rapidly, a line shape for a given speed dependence, but it also permitted us to borrow from and compare with earlier calculations carried out in statistical mechanics. By calculating spectra in various regions of parameter space we were able to reveal the important, but not independent, roles played by the density, relative size of the optical to kinetic cross section and the mass ratio in revealing or concealing the signatures of speed-dependent broadening. We have used physical arguments to support our hypothesis that the conclusions reached are generic and not the result of the specific form chosen for

the speed dependence of the broadening or for the choice of billiard balls (rigid or hard spheres) as a model for the treatment of the translational motion. Being numerical in nature, the work may easily be extended to treat the case where the broadening or shifting is given in numerical form, as will be the case for semiclassical calculations of $\Gamma(v)+i\Delta(v)$. Similarly it will be possible to utilize values of the velocity-changing collision operator generated numerically from a given interaction potential. Consequently we have shown that it is now possible to carry out *ab initio* calculations of the shape of isolated spectral lines starting only from the interaction potential, provided the microscopic scattering calculations are available.

ACKNOWLEDGMENTS

The authors wish to express their gratitude to A. S. Pine for helpful suggestions and advice on programming efficiency. This work was supported by the NSERC Industrial Research Chair in Remote Sounding. One of us (D.A.S.) acknowledges the assistance of Russian Foundation for Basic Research (Grant Nos. 00-02-17973 and 00-15-96808) and Ministry of Industry, Science and Technology.

[1] R. L. Farrow, L. A. Rahn, G. O. Sitz, and G. J. Rosasco, Phys. Rev. Lett. **63**, 746 (1989).
[2] P. Duggan, P. M. Sinclair, A. D. May, and J. R. Drummond, Phys. Rev. A **51**, 218 (1995).
[3] P. R. Berman, J. Quant. Spectrosc. Radiat. Transf. **12**, 1331 (1972).
[4] J. Ward, J. Cooper, and E. W. Smith, J. Quant. Spectrosc. Radiat. Transf. **14**, 555 (1974).
[5] R. H. Dicke, Phys. Rev. **89**, 472 (1953).
[6] L. Galatry, Phys. Rev. **122**, 1218 (1961).
[7] P. Duggan, P. M. Sinclair, R. Berman, A. D. May, and J. R. Drummond, J. Mol. Spectrosc. **186**, 90 (1997).
[8] R. Ciuryło and J. Szudy, J. Quant. Spectrosc. Radiat. Transf. **57**, 411 (1997).
[9] R. Ciuryło and R. Jaworski, J. Jurkowski, A. S. Pine, and J. Szudy, Phys. Rev. A **63**, 032507 (2001).
[10] M. Nelkin and A. Ghatak, Phys. Rev. **135**, A4 (1964).
[11] A. Henry, D. Hurtmans, M. Margottin-Maclou, and A. Valentin, J. Quant. Spectrosc. Radiat. Transf. **56**, 647 (1996).
[12] B. Lance, G. Blanquet, J. Walrand, and J. P. Bouanich, J. Mol. Spectrosc. **185**, 262 (1997).
[13] A. S. Pine, J. Quant. Spectrosc. Radiat. Transf. **62**, 397 (1999).
[14] S. G. Rautian and I. I. Sobelman, Usp. Fiz. Nauk **90**, 209 (1966) [Sov. Phys. Usp. **9**, 701 (1967)].
[15] R. Ciuryło, Phys. Rev. A **58**, 1029 (1998).
[16] B. Lance and D. Robert, J. Chem. Phys. **109**, 8283 (1998); **111**, 789 (1999).
[17] D. A. Shapiro, J. Phys. B **33**, L43 (2000).
[18] R. Ciuryło, A. S. Pine, and J. Szudy, J. Quant. Spectrosc. Radiat. Transf. **68**, 257 (2001); A. S. Pine and R. Ciuryło, J. Mol. Spectrosc. **208**, 180 (2001).
[19] D. A. Shapiro, R. Ciuryło, R. Jaworski, and A. D. May, Can. J. Phys. **79**, 1209 (2001).
[20] J. Keilson and J. E. Storer, Q. Appl. Math. **10**, 243 (1952).
[21] D. A. Shapiro, R. Ciuryło, J. R. Drummond, and A. D. May, Phys. Rev. A **65**, 012501 (2002).
[22] D. Priem, F. Rohart, J. M. Colmont, G. Wlodarczak, and J. P. Bouanich, J. Mol. Struct. **517**, 435 (2000).
[23] M. J. Lindenfeld and B. Shizgal, Comput. Phys. Commun. **41**, 81 (1979).
[24] M. J. Lindenfeld, J. Chem. Phys. **73**, 5817 (1980).
[25] R. C. Desai, J. Chem. Phys. **44**, 77 (1966).
[26] R. C. Desai and M. Nelkin, Nucl. Sci. Eng. **24**, 142 (1966).
[27] J. A. McLennan, *Introduction to Non-Equilibrium Statistical Mechanics* (Prentice Hall, Englewood Cliffs, 1989), p. 117.
[28] D. Robert and L. Bonamy, Eur. Phys. J. D **2**, 245 (1998).
[29] R. Berman, P. M. Sinclair, A. D. May, and J. R. Drummond, J. Mol. Spectrosc. **198**, 283 (1999).
[30] J. W. Forsman, P. M. Sinclair, A. D. May, P. Duggan, and J. R. Drummond, J. Chem. Phys. **97**, 5355 (1992).
[31] S. H. Fakhr-Eslam, G. D. Sheldon, P. M. Sinclair, A. D. May, and J. R. Drummond, Can. J. Phys. **78**, 579 (2000).
[32] H. M. Pickett, J. Chem. Phys. **73**, 6090 (1980).
[33] P. Joubert, X. Bruet, J. Bonamy, D. Robert, F. Chaussard, R. Saint-Loup, and H. Berger, J. Chem. Phys. **113**, 10 056 (2000).
[34] F. Chaussard, X. Michaut, R. Saint-Loup, H. Berger, P. Joubert, B. Lance, J. Bonamy, and D. Robert, J. Chem. Phys. **112**, 158 (2000); F. Chaussard, R. Saint-Loup, H. Berger, P. Joubert, X. Bruet, J. Bonamy, and D. Robert, *ibid.* **113**, 4951 (2000).
[35] E. H. Hauge, Phys. Fluids **13**, 1201 (1970).
[36] A. D. May, Phys. Rev. A **59**, 3495 (1999).
[37] D. A. Shapiro and A. D. May, Phys. Rev. A **63**, 012701 (2001).